Accurate Vision-Based Landing For Multicopter UAVs

CS280: Project Report

Constantin Berzan, Nahush Bhanage, Sunil Shah

Current approaches for automated landing of unmanned aerial vehicles (UAVs) are based on GPS localization, which we show is quite inaccurate. We aim to improve on this by using vision to locate a predefined target, and land on top of it. We describe our progress towards this goal, our approach to pose estimation and control, and the challenges we encountered.

1 Introduction

Multicopter UAVs, colloquially known as *drones*, have become increasingly popular in recent years. This is thanks, in part, to the appearance of affordable prototyping tools (such as the Arduino platform and 3D printers), affordable sensors (such as the accelerometers used in smartphones), and open-source autopilot software (such as ArduCopter by 3D Robotics). Today, a hobbyist can buy an off-the-shelf UAV for less than a thousand US dollars, and get it to fly in only a few hours, using the provided autopilot software.

There is increasing interest in commercial applications of UAVs, such as precision agriculture and package delivery. For these applications to become a reality, the UAVs' operation has to be entirely autonomous, from takeoff to landing. The only approach to autonomous landing for which software is publicly available today is based on GPS. The UAV records its takeoff location, and then navigates back to that location in order to land.

What is the accuracy of GPS-based landing? To find out, we ran the following experiment 10 times: We placed a marker on the ground, placed the UAV on top of it, flew it an arbitrary distance away, and then landed it automatically using ArduCopter's *return-to-launch* mode. We measured the straight-line distance from the marker to the location where the UAV actually landed. We obtained a mean of 195.33 cm and a standard deviation of 110.73 cm. While this might be sufficient when landing in an uninhabited field, it is certainly not sufficient for landing in an inhabited area (for package delivery) or for landing on a charging station (for precision agriculture).

The goal of our project was to improve the accuracy of automated landing by equipping the UAV with a camera, and using computer-vision techniques to guide the UAV towards landing on a predefined marker. We made significant progress towards this goal, although we were not yet able to demonstrate fully autonomous landing. In this document we survey some prior work, present our approach to pose estimation and control, show some accuracy and performance results, and discuss the challenges we encountered. (This work is part of an ongoing project to build an automated charging station for UAVs. Our code is available as open source at `https://github.com/cberzan/drones-287`.)

2 Prior Work

The automated landing problem has been investigated in the research literature of the early 2000s. Here we briefly describe the approaches taken by some of the most cited papers on this topic.

Sharp, Shakernia, and Sastry [**sharp˙et˙al˙2001**] designed an approach for automatically landing an unmanned helicopter. Their landing target uses a simple monochromatic design made up of several squares. Onboard the helicopter, they use a pan-tilt-zoom camera and two embedded computers with Intel CPUs. They discuss the details of their approach to pose estimation, but omit the details of the helicopter controller. Using a real-time OS and optimized custom code, they are able to get their vision system to operate at a rate of 30 Hz.

Our own approach in this project is modeled after that of Sharp et al. The main differences are that (1) we use cheap off-the-shelf hardware, rather than research-grade hardware; (2) our camera is stationary, it is not capable of panning or tilting; and (3) we use off-the-shelf software components such as ROS and OpenCV, rather than writing all of our code from scratch.

Saripalli, Montgomery, and Sukhatme [**saripalli˙et˙al˙2002**] designed another approach for automatically landing an unmanned helicopter. They use a monochromatic H-shaped landing target. Their onboard vision system detects this landing target and outputs the helicopter's relative position with respect to it. This is sent wirelessly to a behavior-based controller running on a ground station, which then directs the helicopter to land on top of the target.

They are able to run their controller at 10 Hz this way. They are also using a high-accuracy differential GPS system, and it is not clear how much their differential GPS and vision systems contribute to a successful landing.

Garcia-Pardo, Sukhatme, and Montgomery [**garcia·pardo·et·al·2002**] look at a more general problem, where there is no pre-specified landing target, and their helicopter has to search autonomously for a suitable clear area on which to land.

3 Our Approach

3.1 Architecture

Our goal was to use inexpensive, off-the-shelf hardware, rather than expensive equipment that is only accessible to researchers. We used quadcopter components made by 3D Robotics, together with their ArduCopter autopilot (frequently referred to under its old name, ArduPilot Mega or APM) and associated GPS module. This autopilot acts as a low-level controller that keeps the quadcopter stable. It runs an unmodified version of the open-source autopilot code provided by 3D Robotics.

We augmented the quadcopter with a BeagleBone Black embedded computer, which uses a 1 GHz ARM CPU. (Since the ARM architecture is so different from x86, the 1 GHz figure should not be compared to the frequency of modern-day Intel CPUs, which are far more advanced, and expensive.) Using a powered USB hub, we connected the autopilot to the BeagleBone. We also connected the webcam and a Wi-Fi adapter this way. Figures **??** and **??** illustrate our complete architecture.

On the BeagleBone, we installed a pre-built image of the Ubuntu 12.04 distribution, obtained from `armhf.com`. We installed pre-built packages for ROS groovy from the official ROS repositories. We compiled OpenCV 2.4.7 by hand. We also installed roscopter, a third-party piece of software that reads the state of the autopilot and makes it available via ROS, and also makes it possible to send controls to the autopilot. Our software took the form of several ROS nodes passing messages to one another. This is illustrated in figure **??**.

3.2 Corner Detection

As a first step, we detect the corners of the landing platform in an image (see Figure **??**):

1. Denoise the image using a 3x3 median filter, and pass it through the Canny edge detector.
2. Identify contours and establish a tree-structured hierarchy among them.
3. Discard contours which are not four-sided convex polygons and which have an area less than an experimentally determined threshold value. We look for four-sided polygons and not specifically for squares, since they will not appear as squares under perspective projection.
4. Using the contour hierarchy, determine a contour which contains 6 other contours. This contour represents the boundary of our landing platform. Store coordinates of the corners of these 6 inner contours.
5. Label the largest of the 6 polygons as 'A' and the farthest one from 'A' as 'D'. Label polygons as 'B', 'C', 'E' and 'F' based on their orientation and distance relative to the vector formed by joining centers of 'A' and 'D'.
6. For each polygon, label corners in anti-clockwise order.

3.3 Pose Estimation

We define the origin of the world coordinate frame to be the center of the landing platform, such that all points on the landing platform have a Z coordinate of zero. The corner detector gives us image coordinates for the 24 corners. Thus, we have a set of 24 point correspondences between world coordinates and image coordinates. Given this input, we want to compute the quadcopter's pose, i.e. the position and orientation of the camera in the world coordinate frame. To do this, we follow the approach of Sharp et al. [**sharp·et·al·2001**], whose details we omit here for brevity. We use SVD to approximately solve a linear system of 48 equations with 6 degrees of freedom.

The output from the pose estimator is a translation vector $t = \begin{bmatrix} t_x & t_y & t_z \end{bmatrix}^\top$ and a 3x3 rotation matrix R. We compute the camera position in world coordinates as $C = -R^\top t$, and the yaw angle as $\alpha = \arctan(R_{21}/R_{11})$. (The roll and pitch angles can be computed similarly, but we do not require them in the control algorithm.)

The approach above assumes a calibrated pinhole camera. For the pose estimates to be meaningful, our camera had to be calibrated first. We calibrated our camera using the `camera_calibration` tool provided in the OpenCV tutorials, plus some manual tuning. We used the resulting calibration matrix to convert the raw pixel coordinates into coordinates for a calibrated pinhole camera model, which we then fed into the equations above.

3.4 Control

We defer real-time control of the UAV to the autopilot's *loiter* mode. This takes care of real-time stabilisation, and attempts to keep the UAV in the same location using GPS. Our vision system then sends small corrections to these controls, guiding the UAV towards the landing platform.

Our controller takes the form of a state machine, illustrated in Figure **??**. The UAV starts out in the *FLYING* state. When landing is desired, it switches into the *SEEK_HOME* state. This uses the autopilot's *return-to-launch* mode to bring the UAV close to the original takeoff location, using GPS. When the landing platform becomes visible, the UAV switches into the *LAND_HIGH* state. Here we use our vision-based pose estimates with a simple proportional controller to guide the UAV towards the landing platform. (The error terms in our controller are given as x, y, z, and yaw deviations. The controller descends at a fixed rate, using the z deviation only as an estimate of the altitude.) When the UAV reaches a predefined altitude (where pose estimates are no longer possible, due to limited field of view), our controller enters the *LAND_LOW* state, and descends slowly by dead reckoning. When the barometric pressure sensor indicates that the UAV has reached the ground, the controller switches into the *POWER_OFF* state.

4 Results

4.1 Pose Estimation Accuracy

We tested the accuracy of our pose estimator in the lab, by holding the camera above the landing pad, and comparing the true measured height to the height reported by the pose estimator. We also measured the standard deviation in our pose estimate, by taking multiple measurements of the same scene. We compared the standard deviation on x and y to the lower bound given by the dimensions on the ground plane that correspond to one pixel in a 640x480 image at a given height. Table **??** shows these results. There is a small (1.4% relative) systematic overestimation of the true height. This can be corrected by doing more precise calibration. The height estimate is very stable at these heights (small standard deviation). The x and y estimates are also fairly accurate, although the error in these estimates is an order of magnitude greater than the lower bound. This is consistent with the fact that there is some noise in the corner detection, and the pose estimator finds an approximate solution. In summary, this experiment suggests that our pose estimates should be good enough to reliably land our quadcopter. If individual measurements are too noisy, it is possible to get better pose estimates using a Kalman filter, although that requires having a model of the dynamics and controls of the system.

true height	z mean	z std	x bound	x std	y bound	y std	yaw std
88 cm	89.3 cm	0.05 cm	0.19 cm	0.43 cm	0.14 cm	0.39 cm	0.12 °
120 cm	121.1 cm	0.08 cm	0.26 cm	1.16 cm	0.19 cm	1.06 cm	0.12 °
170 cm	172.0 cm	0.18 cm	0.37 cm	2.74 cm	0.27 cm	2.17 cm	0.07 °
226 cm	229.0 cm	0.54 cm	0.49 cm	6.51 cm	0.36 cm	6.05 cm	0.34 °

Table 1: Accuracy of our pose estimates. "x bound" and "y bound" are lower bounds for the error on x and y, given by the limited image resolution.

4.2 Performance on the Embedded Computer

When running on a modern-day laptop, our system easily achieves 30 frames per second (FPS), the upper bound dictated by the camera we are using. Unfortunately, performance is much slower on the embedded BeagleBone computer. Just capturing frames from the camera puts significant strain on the system, and we are only able to get 11.2 FPS, even if we perform no processing on the frames. Adding the pose estimation code reduces performance to 3.0 FPS, and running roscopter at the same time further reduces performance to 1.6 FPS.

These disappointing performance numbers point to a fundamental tradeoff when developing a system such as ours: One could use off-the-shelf software packages like ROS and OpenCV, which reduce development time, or one could talk directly to the hardware and write all the code from scratch, which guarantees top performance. Sharp et al [**sharp˙et˙al˙2001**] achieved 30 FPS with their custom-code approach. Our experience suggests that even a decade later, it is impractical to achieve good performance if we rely too much on third-party libraries.

5 Challenges

This section describes the challenges we have encountered, and should be especially helpful to someone trying to replicate or extend our project. We discuss some potential solutions in the next section.

5.1 Platform Integration

We spent an unexpectedly large amount of time addressing integration issues. The first two USB hubs we tried did not work reliably with the BeagleBone, failing to be recognized if they were plugged in at boot time. The first Wi-Fi adapter we tried did not support ad-hoc networking, despite the manufacturer's claims to the contrary. In addition, the hastily written documentation for roscopter mentioned the `--rate` parameter instead of `--baud-rate`, leading to baffling failures to communicate with the APM, until we dug into this third-party code and found the problem.[1]

Another issue was that our webcam tried to automatically adjust exposure and focus, which led to unfocused or over-exposed images in the field. After extensive trial-and-error, we figured out how to tell the hardware to keep the exposure and focus at fixed values, but this required that we run an experiment to determine these values each time we went to fly our quadcopter.

Our main lesson from this experience is that we should not underestimate the amount of time it takes to assemble and validate a new hardware platform for running experiments. It is doubtlessly much quicker to get started with a platform that others have already validated, or to use a software simulation.

5.2 Field of View and Sensor Limitations

We measured our camera's field of view to 69° on the long side and 42° on the short side. This means that at a height of one meter, we see an area of 1.37 m by 0.77 m on the ground. Our landing platform is about 0.76 m by 0.76 m. This means that at a height of one meter, the UAV has to be exactly above the landing pad in order to see all of it. (We get pose estimates only if we see all the corners of the landing pad.) Since the UAV is rarely exactly above the landing platform, the limited field of view is also a problem at heights above one meter.

We thought that we would guide the UAV to a height of one meter using vision, and then land using dead reckoning. The latter turned out to be difficult for two reasons. First, airflow effects near the ground made the motion of the UAV unpredictable. Second, there was a lot of drift in the barometer data, so we were unable to get reliable height estimates below one meter, and thus our controller could not tell when to *POWER_OFF*.

When the landing platform was in sight, we still sometimes failed to detect corners because of blurry images. These are caused by camera shake, and are especially problematic in lower-light conditions such as a cloudy day. Figure **??** shows an example image.

5.3 Weather

Two aspects of weather led to difficulties. First, the cold temperature affected the batteries, reducing flight time to a meager 5 minutes. Second, our controller struggled with gusts of wind. We relied on the autopilot's GPS-based *loiter* mode to keep the UAV in place while the vision system sent small adjustments to the controls. In windy conditions, there was significant drift in *loiter* mode.

6 Future Work and Conclusion

To improve the field of view at low heights, we are considering a modified design for the landing platform. It is also possible to use a fish-eye lens to get a wider field of view. We are also working on a full PID controller, which would provide more aggressive control in windy conditions. It is also critical to optimize our code and hardware stack so that we can get pose estimates at a higher frequency.

Although we were unable to demonstrate an accurate landing using vision, we made significant progress towards this goal. We demonstrated accurate pose estimation using a known landing target, and made our code available online. Although a proof-of-concept demonstration is within reach, our system requires significant testing before it can be used as an off-the-shelf component.

---

[1] We have released a corrected and somewhat cleaned-up version of roscopter at `https://github.com/cberzan/roscopter`.
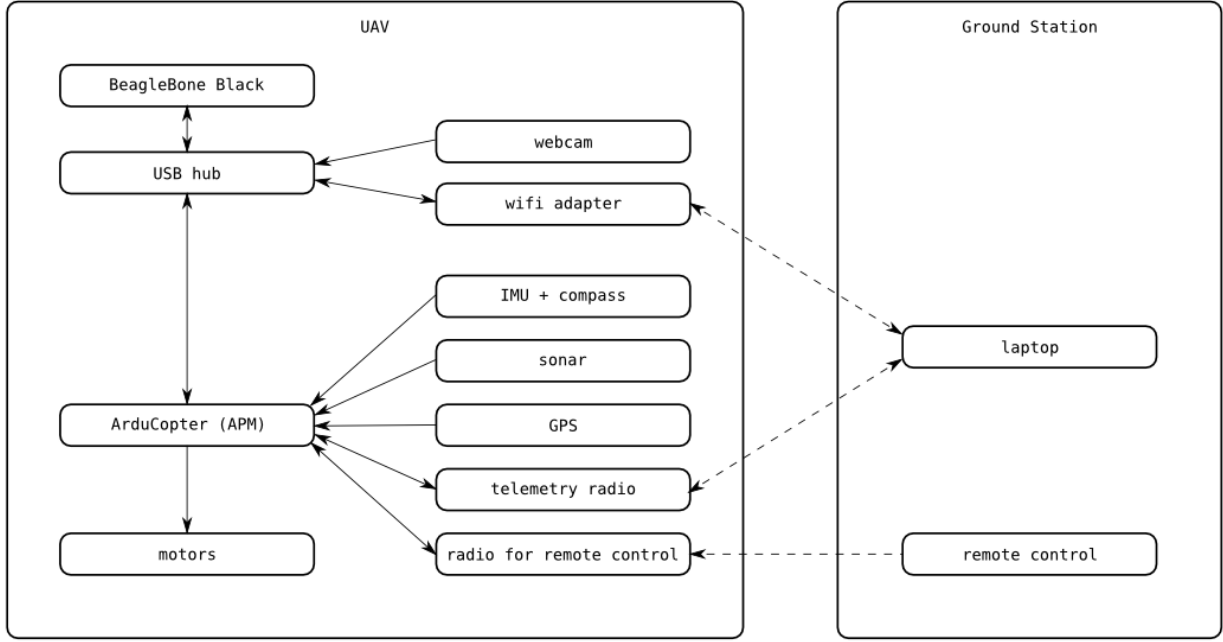
Figure 1: Architecture of our automated landing system. We use inexpensive off-the-shelf hardware. The laptop and remote control are for monitoring and emergency takeover by a human pilot. All the computation is performed onboard the UAV.
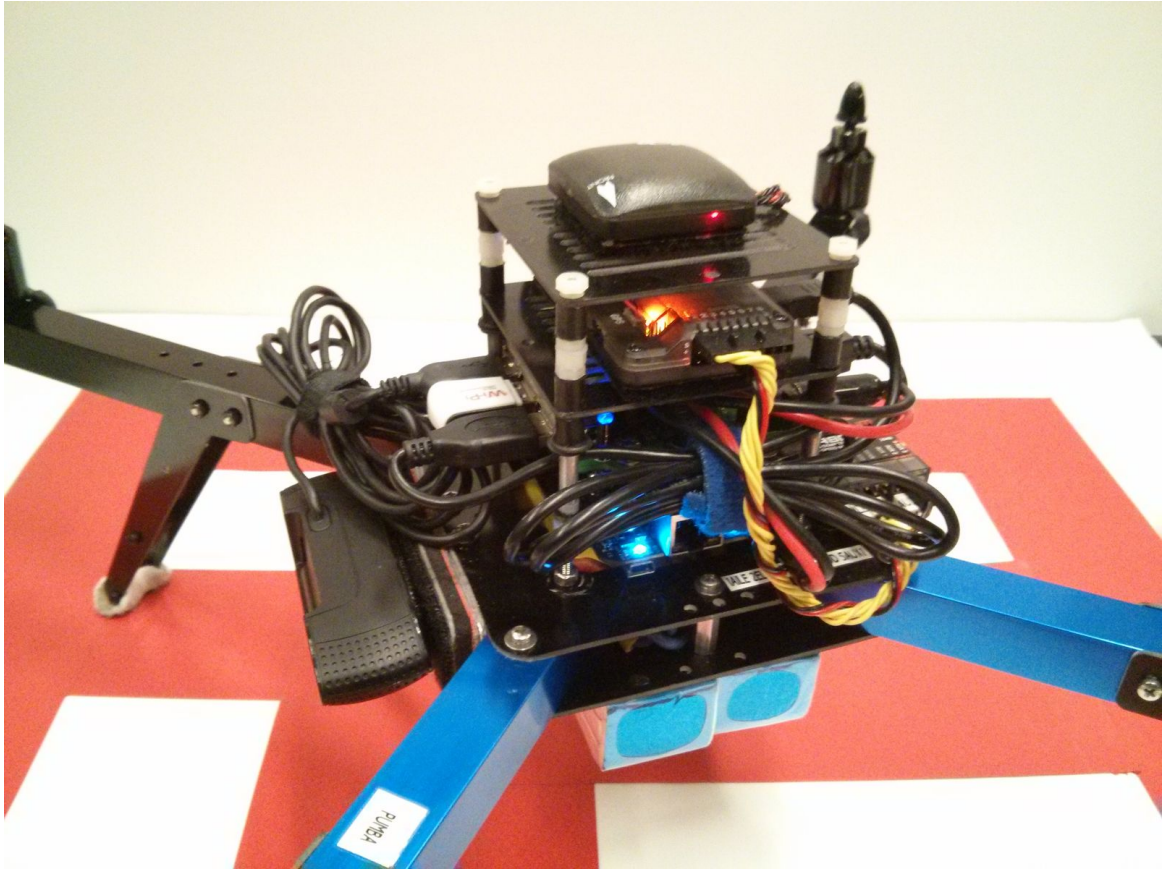

Figure 2: Our hardware stack fully assembled. From bottom to top: batteries, BeagleBone embedded computer, USB hub with Wi-Fi adapter, 3D Robotics autopilot with embedded sensors, GPS module. The webcam is on the left, and the radio for the remote control is on the right. Total weight excluding batteries is 1.35 kg.
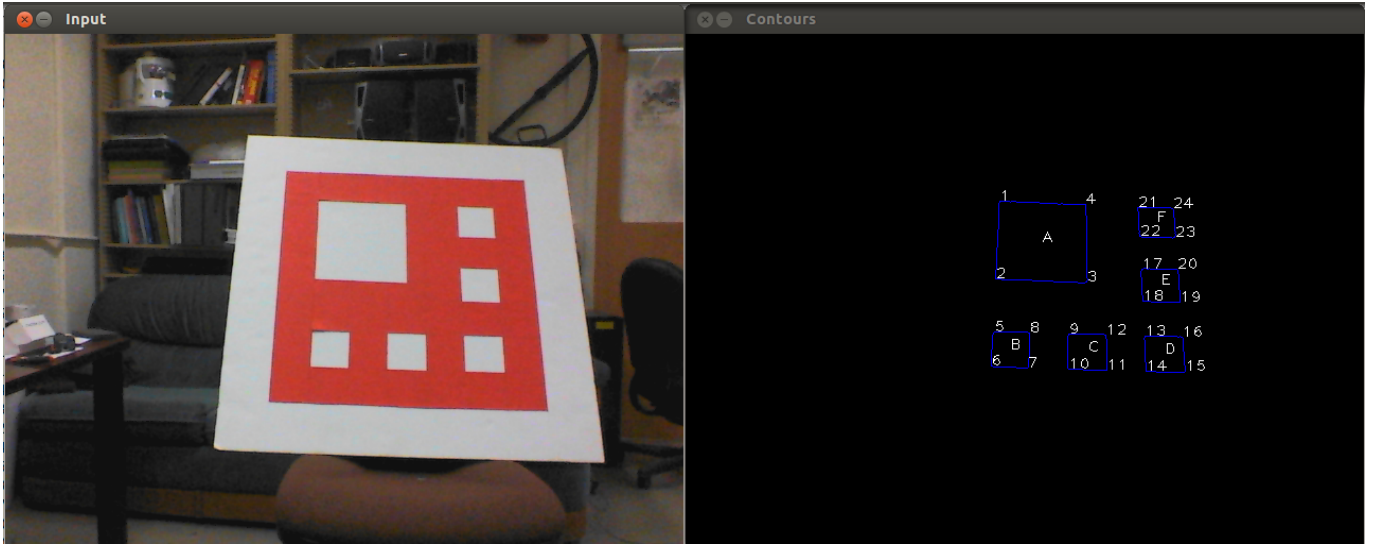
Figure 3: Left: Design of our landing platform. Right: Output of the corner detector (24 points, in order).
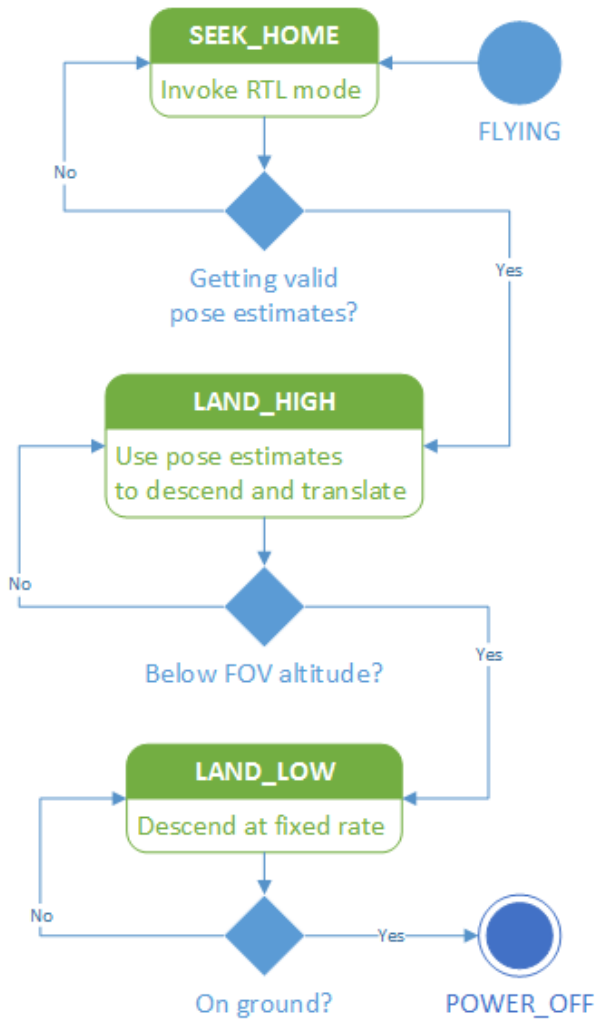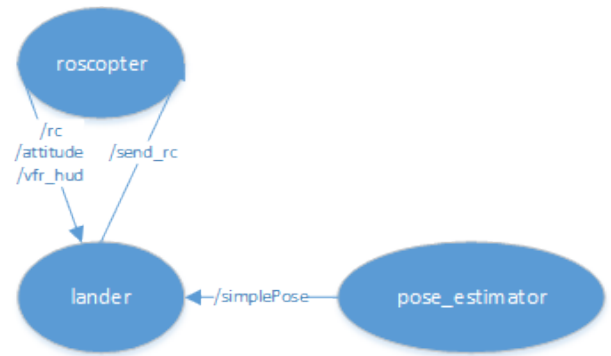

Figure 5: ROS nodes and topics for exchanging messages.

Figure 4: State diagram of our landing controller.

Figure 6: An image where pose estimation fails.